American Mineralogist, Volume 68, pages 143–155, 1983

Exsolution of ilmenite and rutile in hornblende

PANJAWAN MONGKOLTIP AND JOHN R. ASHWORTH

Department of Geological Sciences
University of Aston in Birmingham
Gosta Green, Birmingham B4 7ET, United Kingdom

Abstract

Hornblendes from two basic intrusions in the Caledonian metamorphic terrane of western Scotland contain small (~1 to 10 μm) particles of ilmenite and rutile, exsolved in orientations that are semi-coherent with the amphibole. They were studied by optical microscopy, electron microprobe analysis, scanning and transmission electron microscopy, and X-ray diffraction. Ilmenite occurs in 8 orientations (4 pairs in which members of a pair are equivalent by the symmetry of the hornblende). Rutile occurs in 6 orientations (4 symmetrically distinct orientations). The (0001) plane of ilmenite is approximately parallel to (100), (001), $(\bar{2}61)$, or $(26\bar{1})$ of hornblende ($C2/m$ setting). The c axis of rutile is approximately parallel to [010], [102], [016], $[0\bar{1}6]$, [310], or $[3\bar{1}0]$ of hornblende. Small ilmenite particles are platy parallel to (0001); larger ones tend to develop less simple morphologies. Rutile is usually elongated $\parallel$ c. Strain is accommodated by misfit dislocations in interfaces between oxide and hornblende. The orientations are interpreted in terms of the fully O-rotated model amphibole structure, in which the oxygen atoms are cubic close-packed. A real hornblende structure contains nearly close-packed planes, corresponding to the {111} planes of the cubic close-packed array, and these are the (0001) planes of the hexagonal close-packed oxygen arrays of the oriented ilmenites. The c vector of rutile is related to the linear close-packing in the ⟨110⟩ directions of the cubic close-packed array.

The proportion of ilmenite in one hornblende is estimated at 2.6 volume %, with much smaller amounts of rutile. At the other locality, rutile predominates over ilmenite. It is possible that the ilmenite and rutile were exsolved, in a closed system, from a parental amphibole with a normal structural formula, since slight changes in the total number of cations in the formula can be accommodated by movement of Na between the B sites and the partly vacant A sites. An analysis of an ilmenite particle indicates approximately 6 mole % Fe_2O_3, and a fine structure seen in transmission electron micrographs is attributed to incipient exsolution of hematite from the ilmenite.

Introduction

Oxide inclusions in amphiboles have been neglected by comparison with those in pyroxenes, where the identification of oriented spinel-group minerals and ilmenite (Bown and Gay, 1959) has been followed by the description of rutile (Moore, 1968; Griffin *et al.*, 1971). Fleet *et al.* (1980) present a detailed study of magnetite in pyroxene, and the origin of ilmenite and spinel lamellae in pyroxene is assessed by Garrison and Taylor (1981).

Although oxide particles in hornblende have been noticed in passing (*e.g.*, Fleet *et al.*, 1980), to the best of our knowledge there has been no thorough investigation. Since it is generally accepted that the Ti content of hornblende tends to increase with increasing temperature of equilibration (Leake, 1965; Bard, 1970; Helz, 1973; Raase, 1974), exsolution of Ti minerals might be expected during the cooling of some hornblendes. In this paper, we infer this origin for oriented ilmenite and rutile particles in hornblendes from two slowly cooled intrusions in the western Highlands of Scotland.

Geological setting

Two rocks were studied, both from basic intrusions. One is from the Glen Scaddle basic igneous mass at National Grid reference NM 983 685. This metagabbroic intrusion pre-dates the main Caledo-

0003–004X/83/0102–0143$02.00

nian deformation of the region, during which its mineralogy was affected by metamorphism (Stoker, 1980). The occurrence of inclusions in hornblende is unusual in this intrusion; the rock studied also has unusually abundant, Ti-rich amphibole, and lacks pyroxene. It probably belongs to the minor component of the intrusion termed "appinite" by Drever (1940). "Appinite" is a local name for a hornblende-rich meladiorite (Hatch *et al.*, 1972, p. 310). The other specimen is also "appinitic," and is from Grid reference NN 131 831, in the Glen Loy intrusion, which is of Caledonian synorogenic age (Institute of Geological Sciences, 1975).

Petrography

In both rocks hornblende is the major mineral, with some plagioclase, and small amounts of chlorite, titanite and ilmenite. Oriented inclusions are abundant in the interiors of hornblende grains (Fig. 1). The color of the inclusion-bearing hornblende is generally green. Some interior parts of grains are brown, and these usually lack inclusions. Among the inclusions from Glen Scaddle, which range from 1 to 10 μm in longest dimension, brown plates can be distinguished from less strongly colored, rod-like to acicular particles. In the Glen Loy specimen, both the hornblende and its inclusions are finer-grained, and the inclusions are mostly acicular.

Scanning electron microscopy (SEM)

SEM of polished surfaces, combined with qualitative analysis by energy-dispersive X-ray detector, was used to assess the relative abundances of two types of particle, distinguished by their contrast in electron images and their major elements with atomic number greater than 8 (Fig. 2). One type of inclusion gave a Ti peak only, the other, both Ti and Fe (Fig. 2a). Anticipating the transmission electron microscopy (TEM), these can be identified as rutile and ilmenite respectively. The ilmenite forms the brown plates, and the rutile the rods and needles, seen optically. In electron images, they were most easily distinguished by using an annular silicon diode detector of the type developed by Hall and Lloyd (1981) for back-scattered electrons. This gives strong atomic number contrast (Fig. 2b). Using a conventional, commercial instrument (Cambridge Instruments Stereoscan S150), the two minerals could be clearly distinguished in X-ray scanning images (Fig. 2d,e), but this was tedious, and we found that sufficient contrast was obtained from the conventional electron detector for the distinction to be made in electron images (Fig. 2c).

It was found that most of the inclusions in the Glen Scaddle hornblendes were ilmenite, only a few percent being rutile, while rutile predominates over ilmenite in the Glen Loy material. The two minerals were usually found as separate grains scattered through the host amphibole, though intergrowths were occasionally seen (Fig. 2c), as were small arrays of particles (Fig. 2b).

Electron microprobe analysis

It was generally difficult to avoid inclusions when analyzing these amphiboles. However, in the Glen Scaddle material, it was possible to analyze an area of hornblende among the inclusions (Table 1, Analysis 1) and, separately, an ilmenite inclusion (Analysis 4). Tabulated for comparison are data from an inclusion-free, brown area of the same amphibole grain (Analysis 2), and a primary ilmenite (Analysis 3). The inclusion and the primary ilemnite are very

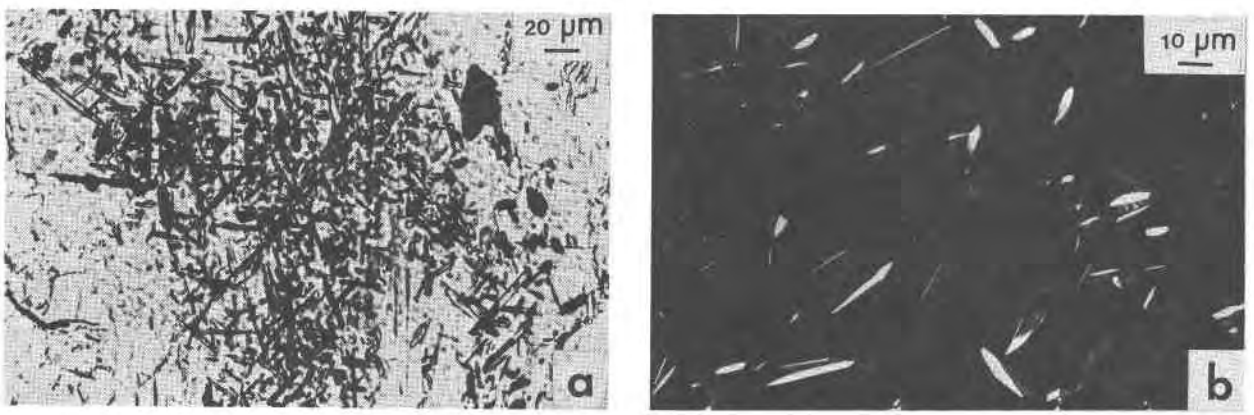

Fig. 1. Optical photomicrographs showing inclusions in hornblende from Glen Scaddle. (a) Transmitted, plane-polarized light. (b) Reflected light.

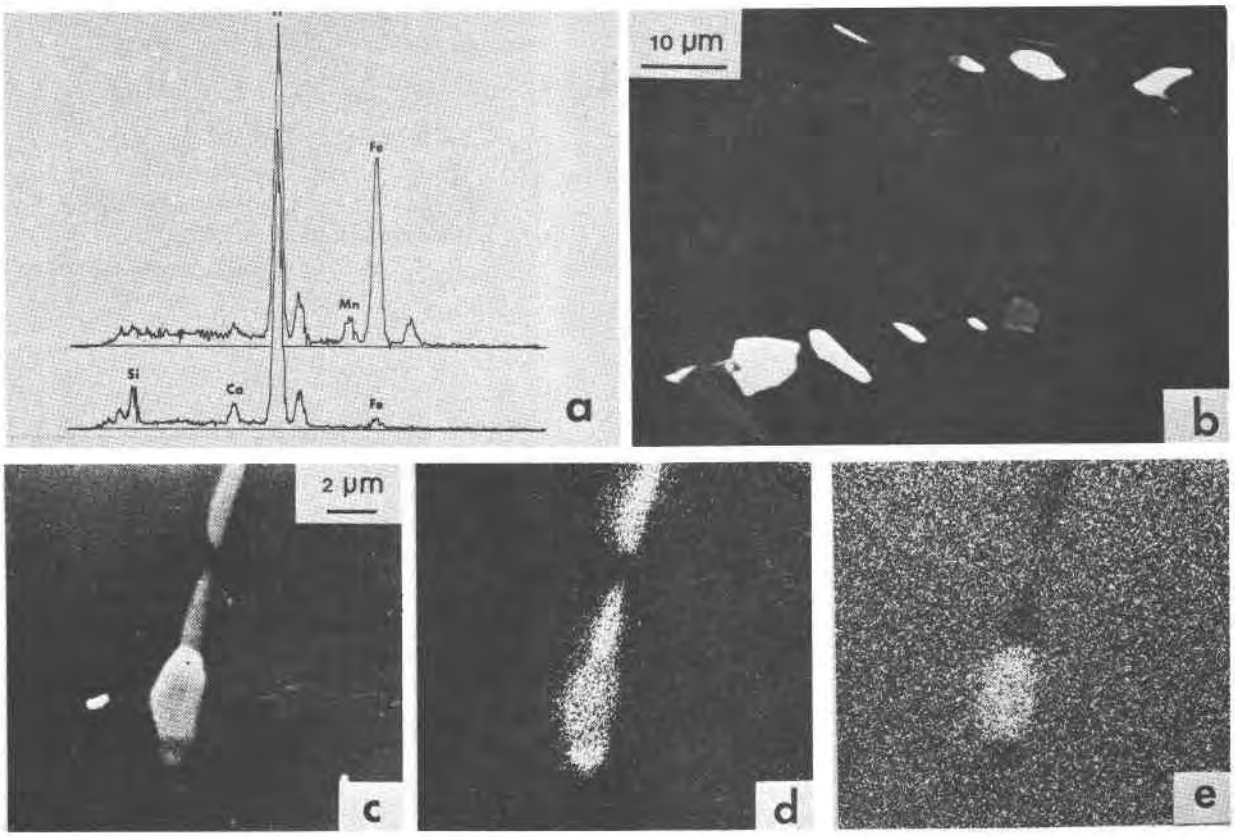

Fig. 2. SEM observations of inclusions. (a) Energy-dispersive X-ray spectra from an ilmenite inclusion (top) and a rutile inclusion. The rutile spectrum is slightly contaminated by the host hornblende, giving Si, Ca and Fe peaks. (b) Electron image obtained with a semiconductor detector for back-scattered electrons (Hall and Lloyd, 1981). There is strong atomic number contrast between ilmenite (white) and rutile (grey). Hornblende is black. In this area the inclusions are spatially arranged in two arrays. (c) Electron image from conventional detector, photographed and printed under the same conditions as (b): contrast is poorer, but ilmenite is still distinctly brighter than rutile. (d) and (e) X-ray images of same area as (c); (d) Ti X-rays, (e) Fe X-rays.

similar in composition. Both contain approximately 6 mole % Fe_2O_3 in solid solution. Inclusion-free green rims of hornblende grains are similar in Ti content to the tabulated green hornblende (Analysis 1). The high Ti of the inclusion-free, brown, internal area (Analysis 2) is explicable by the failure of ilmenite to develop there, but the composition of the brown area is not simply that of the green inclusion-bearing hornblende (Analysis 1) plus its inclusions, since the Fe content is almost exactly the same in Analyses 1 and 2. The amphibole must originally have been zoned, an effect which also accounts for the green, inclusion-free rims. In the Glen Loy material, these rims again have lower Ti (Analysis 7) than the bulk of the grain (Analysis 6). Here it was not possible to obtain good analyses of amphibole interiors without having some of the very small inclusions in the beam; the data for inclusion-bearing amphibole thus represent hornblende plus rutile inclusions. If the inclusions are exsolution products, this analysis should serve as an estimate of a primary amphibole composition. In 42 analyses from this rock, there is a strong inverse correlation between Ti and Si (Fig. 3). The correlation coefficient is −0.719, which is significant at the 0.1% level. The overall substitution is probably Ti + Al^{IV} for Si + Al^{VI}. This effect indicates that Ti in the primary amphibole did not simply represent solid solution towards a TiO_2 end-member, despite the subsequent production of predominantly TiO_2 inclusions.

In the I.M.A. nomenclature of amphiboles (Leake, 1978), the name hornblende is correct for the pure analyses (1, 2, and 7 in Table 1). In the recalculations of analyses contaminated by inclusions, high Ti values are associated with Si < 6.25 (Table 1, Analysis 6; Fig. 3): if, as suggested above, these represent primary amphiboles, they should be

Table 1. Electron microprobe analytical data

Locality	Glen Scaddle					Glen Loy	
Mineral	amphibole		ilmenite		amphibole		
Analysis No.*	1	2	3	4	5	6	7
SiO_2	42.19	41.93	-	-		41.76	42.91
TiO_2	1.56	2.46	49.41	49.56		3.52	2.56
Al_2O_3	13.15	12.86	-	-		12.53	12.78
FeO**	13.82	13.89	48.76	47.88		12.05	11.92
MnO	0.18	0.17	1.05	1.36		0.22	0.17
MgO	11.91	11.70	0.12	0.05		13.46	13.73
CaO	11.62	11.51	0.02	0.19		11.47	11.25
Na_2O	1.94	1.91	-	-		2.44	2.58
K_2O	0.67	0.67	-	-		0.70	0.58
$H_2O^{\dagger}$	2.01	2.01	-	-		2.04	2.06
Total	99.05	99.11	99.36	99.04		100.19	100.54
Formula to	23 oxygens		to 6 oxygens		to 23 oxygens		
Si	6.29	6.26	-	-	6.12	6.14	6.26
Al^{IV}	1.71	1.74	-	-	1.88	1.86	1.74
Al^{VI}	0.61	0.52	-	-	0.38	0.31	0.45
Ti	0.18	0.28	1.88	1.89	0.39	0.39	0.28
Mg	2.65	2.60	0.01	0.00	2.58	2.95	2.98
Fe^{2+}	1.72**	1.73**	1.83	1.82	1.89**	1.48**	1.45**
Fe^{3+}	-	-	$0.24^{\dagger\dagger}$	$0.22^{\dagger\dagger}$	-	-	-
Mn	0.02	0.02	0.05	0.06	0.02	0.03	0.02
Total	13.18	13.15			13.26	13.16	13.18
Na	0.56	0.55	-	-	0.54	0.70	0.73
Ca	1.86	1.84	0.00	0.01	1.81	1.81	1.76
K	0.13	0.13	-	-	0.13	0.13	0.11
Total	2.55	2.52			2.48	2.64	2.60

** 1: green amphibole associated with ilmenite inclusions. 2: brown, inclusion-free area of the same amphibole grain. 3: primary ilmenite. 4: ilmenite inclusion in amphibole. 5: reconstructed composition of amphibole (1) prior to exsolution of 2.8% ilmenite. 6: amphibole plus rutile inclusions. 7: inclusion-free edge of the same amphibole grain.*
*** total Fe as FeO.*
†H_2O calculated from ideal formula with 22 O and 2 OH.
††Fe^{3+} in ilmenite estimated from stoichiometric constraints.

called ferroan pargasite, or magnesio-hastingsite if Fe^{3+} exceeds Al^{VI}. We cannot reliably estimate Fe^{3+}. Since our cation totals excluding (Na + Ca + K) considerably exceed 13 (Table 1), recalculation of this total to 13 as suggested by Leake (1978) would indicate substantial Fe^{3+}, very close to the amount of Al^{VI}: averages are, for Glen Scaddle (10 analyses) Fe^{3+} 0.58, Al^{VI} 0.54, Glen Loy (42 analyses) Fe^{3+} 0.46, Al^{VI} 0.45. However, this calculation gives a *maximum* Fe^{3+} content (Stout, 1972), by assuming that Fe^{2+} and Mg are confined to the C sites of the amphibole structural formula $A_{0-1}B_2C_5T_8O_{22}(OH)_2$. Our raw cation totals including Ca, but excluding (Na + K), are always close to 15: means and standard deviations are 15.06±0.06 for Glen Scaddle and 14.91±0.04 for Glen Loy, suggesting that the B, C and T sites are almost fully occupied by the cations other than Na and K, with the amount by which Ca is less than 2 representing Fe and Mg in the B site (solid solution towards cummingtonite). In this case, there need not be substantial Fe^{3+} (Stout, 1972). Thus, we regard the amphiboles as pargasitic rather than hastingsitic: the analyses of pure amphiboles (1, 2, and 7 of Table 1) are ferroan pargasitic hornblendes, while Analysis 6, of amphibole plus inclusions, suggests that the primary titanian amphibole was a ferroan pargasite.

Volume proportion of ilmenite inclusions in a hornblende

The relatively large sizes of the ilmenite plates in the Glen Scaddle hornblende made it feasible to estimate their amount. The SEM study had shown that the amount of rutile is negligible. Two hornblende grains were selected; one was that analyzed in Table 1, and the other gave very similar analyses. Reflected-light photomicrographs were taken of 7 areas, each approximately 150 μm × 100 μm, containing evenly scattered particles. The images were analyzed by using a digitizer to record the positions of particle boundaries, and a microcomputer to convert these to modal proportions. The proportion of inclusions ranged from 1.99 to 3.34%, averaging 2.60% (with a standard error $\sigma = 0.22\%$). This is a minimum estimate, since very small particles (seen in the TEM study) may not be resolved in an optical photomicrograph, but these probably contribute only a small additional volume of ilmenite. Since the oxygen atoms are more closely packed in ilmenite than in hornblende, the proportion on a constant-oxygen basis is slightly higher (2.8% rather than 2.6%). This estimated proportion is used to reconstruct the hypothetical hornblende

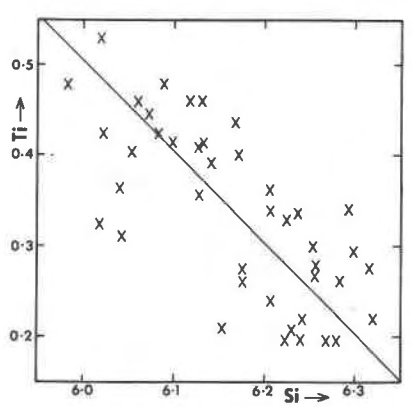

Fig. 3. Ti and Si per 24 (O,OH) in electron microprobe data from Glen Loy amphiboles. The straight line is the least-squares best fit to the data.

composition prior to exsolution of the ilmenite (Table 1, Column 5). Like the Glen Loy analysis of amphibole plus inclusions (Column 6), this is a titanian ferroan pargasite. Since this calculation gives a reasonable amphibole composition, it is plausible to suggest that the inclusions were produced by exsolution in a closed system. Constraints placed on this process by the hornblende structural formula are discussed below.

Orientational relations between hornblende and inclusions

Universal-stage measurements

In Glen Scaddle hornblende, swarms of ilmenite plates with rather consistent orientation (*cf.* Fig. 1) were oriented using a four-axis universal stage. There were uncertainties due to small sizes and irregular shapes of some particles, but consistent features emerged (Fig. 4). There are concentrations of plate–normals near *c*, *b*, and *a** of the hornblende. Most other plate-normals are in hkl and $\overline{hkl}$ positions, rather than hkl and $h\bar{k}l$. The distinction between hkl and the corresponding $\overline{hkl}$ is, of course, arbitrary; the left and right halves of Figure 4 are related by the (010) mirror plane of the hornblende, and a plate–normal is as likely to be found on one side as the other (this is an instance of the "intergrowth symmetry principle" of Bown and Gay, 1959). Thus the differences between the two halves of Figure 4 are merely statistical fluctuations; even allowing for this, there is considerable scatter, which exceeds measurement errors and implies statistical variations in the morphological development of those particles that are coarse enough to be measured optically. In order to study smaller particles and to assess lattice orientation rather than morphology, transmission electron microscopy and X-ray diffraction studies were undertaken.

Transmission electron microscopy

Selected parts of doubly polished thin-sections of both rocks were mounted on titanium mesh support grids and thinned by ion bombardment. TEM was carried out at high voltage (1 MV), with the advantage that thick foils could be studied, enabling relatively large areas to be surveyed. A double-tilt stage was used. Minerals, and their orientational relations, were identified from electron diffraction patterns. The *C*2/*m* setting of hornblende was used, and ilmenite was set on hexagonal axes. All oxide

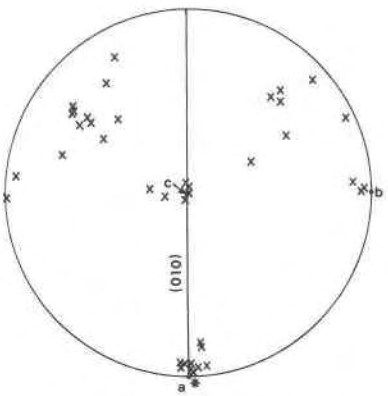

Fig. 4. Poles of ilmenite plates in Glen Scaddle hornblende, measured by universal-stage microscopy. Upper-hemisphere stereogram, with hornblende in *C*2/*m* setting.

particles were identified as either rutile or ilmenite. No other mineral was found as simple inclusions, but the Glen Scaddle hornblende is patchily altered to chlorite and extensively cracked; these effects show no spatial relationship to the oxide inclusions.

Ilmenite particles, ~1 μm in size, are abundant in the Glen Scaddle hornblende (Fig. 5a). They are platy, the habit plane being (0001). They are clearly related crystallographically to the host mineral, the (0001) plates lying parallel to four planes in the amphibole, (100), (001), $(\bar{2}61)$, and $(2\bar{6}1)$. The last two are indistinguishable from their opposites, respectively $(2\bar{6}\bar{1})$ and $(\bar{2}6\bar{1})$. Thus there are only two physically distinct orientations of the form $\{\bar{2}61\}$.

All four orientations can be found close together, but there is a tendency for one of them to predominate within areas of a size ~100 μm^2. For each (0001) orientation, two sets of a_1, a_2, a_3 axes of ilmenite are found. Thus, 8 ilmenite lattice orientations are recognized, but these form pairs related by the symmetry of the hornblende, so that 4 symmetrically distinct sets of ilmenite axes are identified (Table 2). The coincidence between (0001) of ilmenite and the stated lattice plane of hornblende is often exact, within the limits of angular measurement in electron diffraction (~0.5°), as illustrated in Figure 6a, though in other cases discordances of ~1° were noticed. The tabulated coincidences for a_1, a_2, a_3 of ilmenite are necessarily approximate because the angles between the stated hornblende vectors are not exactly 120°. Coincidences with directions lying in (010) of hornblende are generally close except in the $\{\bar{2}61\}$ type of ilmenite, where there is usually a discordance of a few degrees between the [102] zone axis of hornblende and the ilmenite $\langle 1\bar{1}0\rangle$ zone axis with which it would ideally coincide (Fig. 6b).

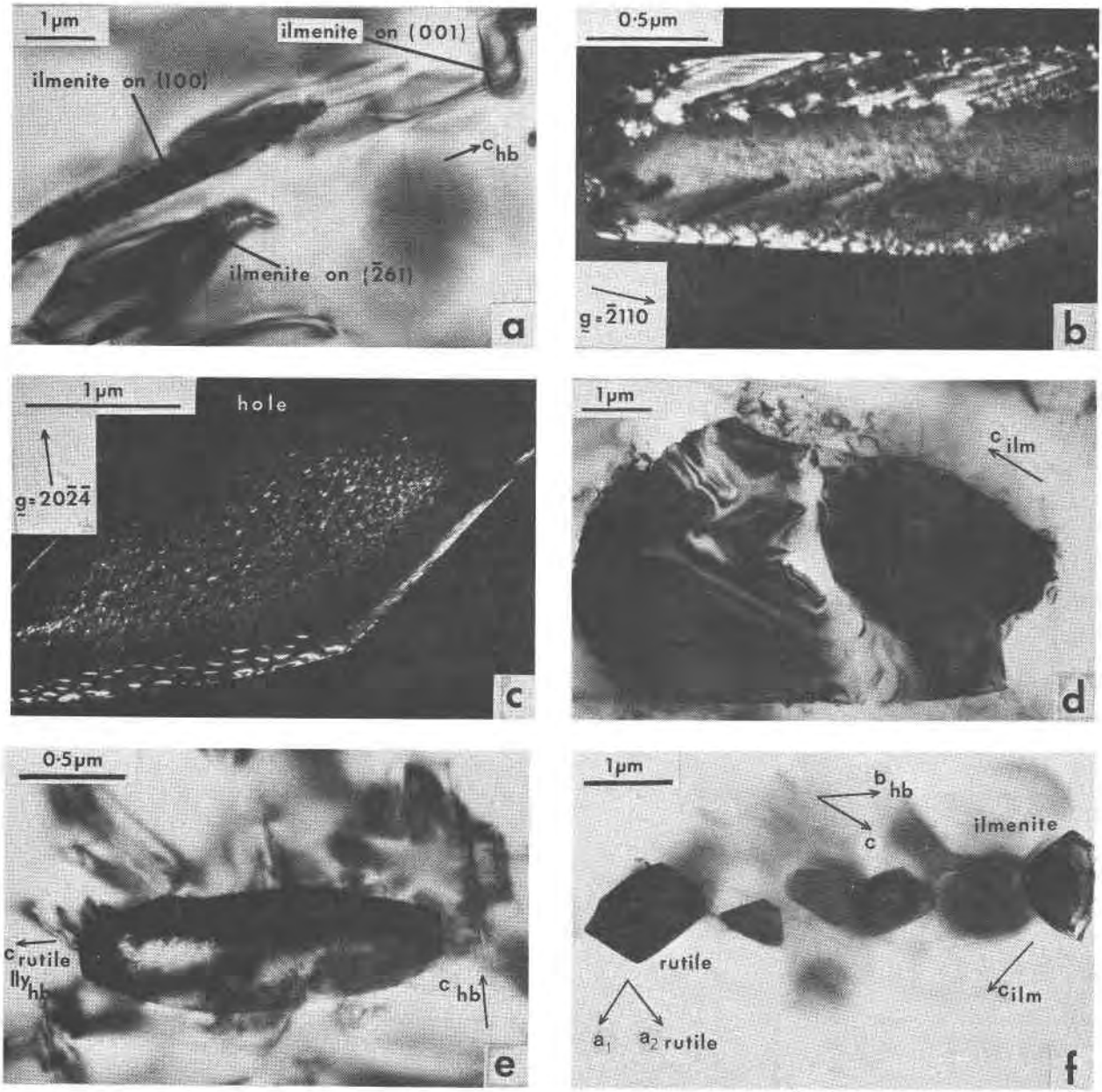

Fig. 5. TEM micrographs of inclusions in hornblende from Glen Scaddle. (a) Ilmenite plates in three different orientations, with (0001) parallel to indicated planes of hornblende. Dislocations are also seen in the hornblende, mostly parallel to c. Viewed approximately along [110] of the hornblende. (b) Ilmenite particle showing misfit dislocations in the (0001) interfaces with hornblende. Dark field image obtained from diffraction vector $\mathbf{g} = \bar{2}110$. (c) Ilmenite plate imaged in dark field using diffraction vector $20\bar{2}\bar{4}$ with the $h,0,\bar{h},2\bar{h}$ row generally excited: viewed approximately along [$2\bar{2}1$]. Substructure in the plate is clearly seen in its thin edge, adjacent to the hole (top) produced by ion bombardment. Dislocations, due to misfit with the host hornblende, produce contrast in the prism faces of the ilmenite. (d) A single large ilmenite particle, showing irregular shape though the lattice is in $\{\bar{2}61\}$ orientation. (e) Rutile particle, viewed along its [210] zone axis, which lies close to [101] of the hornblende. (f) An array of particles. The projected directions of some crystallographic vectors are indicated. Viewed approximately along [114] of the hornblende.

Misfit dislocations, due to the lack of complete coherence between the two structures, are observed in the interfaces (Fig. 5b,c).

The largest ilmenite particles that can be observed by TEM retain the approximate lattice relation to the host, but lack the platy morphology of the small particles, tending to be irregular in shape (Fig. 5d).

Table 2. Approximate orientational relations between hornblende and ilmenite*

Hornblende directions approximately parallel to: $(0001)_{ilm}$	$\underline{c}_{ilm}$	$\underline{a}_1, \underline{a}_2, \underline{a}_3$ ilm	ilm. zone axis approx. $\parallel \underline{c}_{hb}$
(1 0 0)	1 0 0	[0 1 2],[0 $\bar{1}$ 2],[0 0 $\bar{1}$]	[1 1 0]
	$\bar{1}$ 0 0	[0 1 $\bar{2}$],[0 $\bar{1}$ $\bar{2}$],[0 0 1]	[$\bar{1}$ $\bar{1}$ 0]
(0 0 1)	0 0 1	[$\bar{1}$ 1 0],[$\bar{1}$ $\bar{1}$ 0],[1 0 0]	[1 1 1]
	0 0 $\bar{1}$	[1 1 0],[1 $\bar{1}$ 0],[$\bar{1}$ 0 0]	[$\bar{1}$ $\bar{1}$ $\bar{1}$]
{$\bar{2}$ 6 1}	$\bar{2}$ 6 1	[6 1 6],[$\bar{3}$,1,$\bar{12}$],[3 $\bar{2}$ 6]	[$\bar{2}$ $\bar{6}$ 1]
	2 6 $\bar{1}$	[$\bar{6}$ 1 $\bar{6}$],[3,1,12],[3 $\bar{2}$ $\bar{6}$]	[2 6 $\bar{1}$]
	$\bar{2}$ 6 1	[$\bar{6}$ $\bar{1}$ $\bar{6}$],[3,$\bar{1}$,12],[3 2 $\bar{6}$]	[2 6 1]
	2 6 $\bar{1}$	[6 $\bar{1}$ 6],[$\bar{3}$,$\bar{1}$,$\bar{12}$],[$\bar{3}$ 2 6]	[$\bar{2}$ $\bar{6}$ $\bar{1}$]

The ilmenite orientations are arranged in pairs that are equivalent by the symmetry of the hornblende

Table 3. Approximate orientational relations between hornblende and rutile

Hornblende directions approximately parallel to: $\underline{c}_{rutile}$	$\langle 1\ 1\ 0 \rangle_{rutile}$
[0 1 0]	[1 0 2],[$\bar{1}$ 0 2]
[1 0 2]	[0 1 0],[$\bar{1}$ 0 2]
* [$\bar{3}$ 1 0]	[0 $\bar{1}$ 6],[3 2 6]
[$\bar{3}$ $\bar{1}$ 0]	[0 1 6],[3 $\bar{2}$ 6]
* [0 1 6]	[$\bar{3}$ $\bar{1}$ 0],[3 $\bar{2}$ 6]
[0 $\bar{1}$ 6]	[$\bar{3}$ 1 0],[3 2 6]

pair related by hornblende symmetry

Ilmenite often contains a fine substructure (Fig. 5b,c). This can sometimes be resolved into particles of finite size (Fig. 5c) which are associated with strain fields. They occur inside the ilmenite grains rather than being associated with boundaries, an observation confirmed by their presence at a thin edge of ilmenite where there is no overlapping hornblende (Fig. 5c). They are interpreted as exsolved platelets, presumably of hematite; coarser, lenticular particles of exsolved hematite in ilmenite are described by Lally *et al.* (1976). This interpretation is consistent with the inference, from the electron microprobe data, that the ilmenite contains Fe^{3+}. The platelets are often absent from a region near the interface with hornblende (Fig. 5c), suggesting that the ilmenite was zoned, the early-formed central part being richer in Fe^{3+}.

Rutile particles are usually elongate along the *c* axis (Fig. 5e), but otherwise variable in shape. Their approximate orientational relations to hornblende are given in Table 3. These relations are less exact than for ilmenite, variations up to 7° having been noticed between the lattices of adjacent particles in the same nominal orientation. In the simplest orientation, *c* of rutile is parallel to *b* of hornblende (Fig. 6c), while the ⟨110⟩ directions of rutile are less clearly related to the host, the one nominally parallel to [102] tending to be displaced approximately 7° from [102] towards *a* of hornblende with the effect that a ⟨100⟩ axis of rutile is approximately, but not exactly parallel to c^* of the hornblende. The misfit

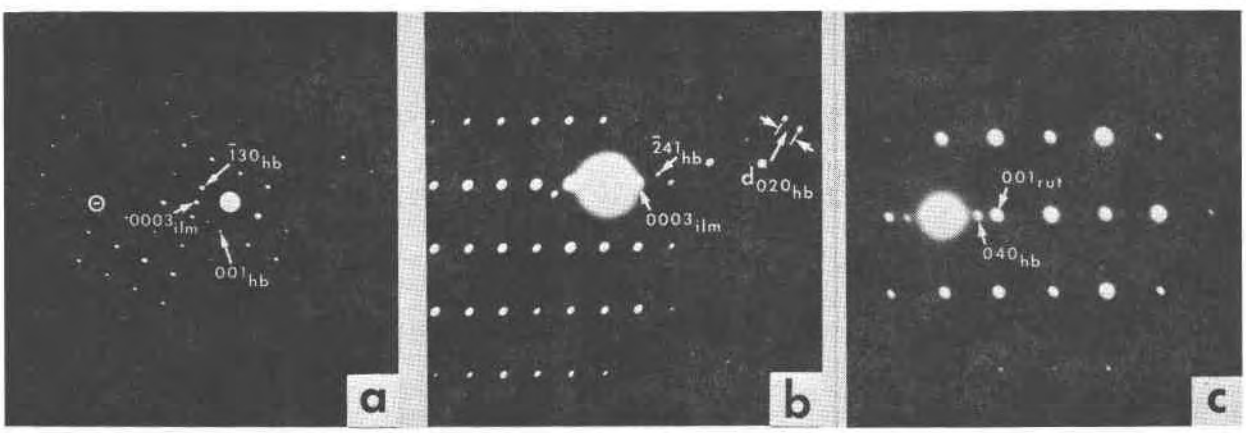

Fig. 6. Electron diffraction patterns of particles and host hornblende. (a) Glen Loy, (b) and (c) Glen Scaddle. (a) [310] zone of hornblende with 000*l* row of ilmenite. This row is parallel to the $\bar{2}61$ reciprocal-lattice vector of the hornblende, but the distances d^*(0006)(ilm) and $d^*(\bar{2}61)$(hb) are slightly different, so that the $\bar{4}$,12,2(hb) and 0,0,0,12(ilm) maxima are resolved (ringed spots). (b) [$1\bar{1}0$] zone from ilmenite of {$\bar{2}61$} orientation type, with arcs of spots from the off-center hornblende zone [102], which would be centered along with the ilmenite zone if the structural coincidence between the two minerals was ideal. (c) [210] zone of the rutile particle of Fig. 5e, with 0*k*0 row of hornblende. The *c* axis of the rutile is approximately parallel to *b* of hornblende, but the two **d*** vectors are not commensurate.

between the rutile and hornblende lattices gives confused contrast in boundaries, sometimes resolvable into networks of dislocations. Other dislocations usually emanate from rutile boundaries into the adjacent hornblende (Fig. 5e).

Where the inclusions form small arrays (Fig. 5f), the orientational relations remain valid. It is not obvious what causes some particles to be arranged in these arrays. No subgrain boundaries (dislocation arrays) were detected in the hornblende, but nucleation of the particles may have been assisted by some such feature, subsequently obscured by dislocation movement due to a deformation which produced the scattered dislocations (Fig. 5) and cracks throughout the hornblende.

X-ray diffraction

Single-crystal oscillation photographs were taken of a hornblende crystal from Glen Scaddle, to check the consistency of ilmenite lattice orientations throughout a larger volume than could be sampled by TEM. The oscillation axis was c, and various centers were used for the oscillation range of 20°. The center of oscillation for each photograph was checked by indexing the hornblende spots. Ilmenite spots were indexed using computer-generated tabulations of ξ and ζ for all the lattice orientations deduced from the TEM work, and bearing in mind the constraints due to the restricted oscillation range. For each ilmenite orientation, a rational zone axis of ilmenite approximately coincides with c of hornblende (Table 2, last column), so that ilmenite layer-lines were found on the photographs (Fig. 7), having spacings ζ differing from that of the hornblende and characteristic of the type of ilmenite orientation, *i.e.*, (100), (001), or {261}. Approximately equal numbers of spots were found for each of these, and all 8 full orientations of Table 2 were confirmed. The spots are sharp, indicating consistent ilmenite orientation, though there are deviations from ideally straight layer-lines, confirming slight deviations from the ideal coincidence between c of hornblende and a simple zone axis of ilmenite.

In all orientations of rutile, the c axis of hornblende represents an irrational direction, so rutile layer-lines were not found, but some isolated spots were identified as being from rutile in the expected approximate orientations.

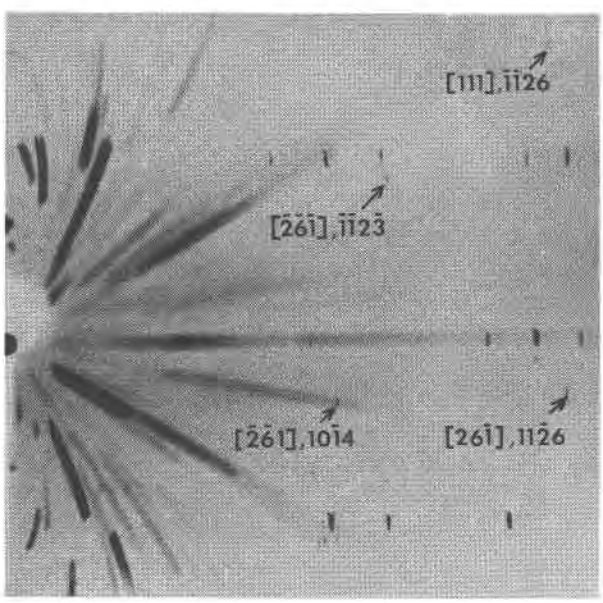

Fig. 7. X-ray oscillation photograph of hornblende from Glen Scaddle, Cr$K\alpha$ radiation. Oscillation axis c(hb), center of oscillation 35° from b^* towards $-a^*$. The strongest ilmenite spots are labelled with the appropriate oscillation axis (Table 2, last column) and their indices.

Interpretation of results

Orientational relations

Ilmenite. The observed orientations can be interpreted in terms of the arrangement of oxygen atoms. In ilmenite this is based on hexagonal close packing. The oxygens in hornblende are not close-packed, but nearly close-packed planes can be identified using a theoretical model of the amphibole structure. This is the "fully O-rotated" structure in the notation of Thompson (1970), where "rotation" refers to the deviation of the double chain of SiO_4 tetrahedra from a fully extended state. The hornblende ($C2/m$ amphibole) structure is, in fact, *partly* O-rotated (Cameron and Papike, 1979). This leads to closer packing of the oxygens than in the theoretical fully extended structure and, indeed, the fully O-rotated structure would have cubic close-packed oxygens. The amphibole structures are treated in terms of oxygen packing by Law and Whittaker (1980). The relations between lattice vectors of the close-packed $C2/m$ model amphibole and those of the cubic close-packed oxygen sub-lattice are: $\mathbf{a}_{amph} = [121]_{ccp}$, $\mathbf{b}_{amph} = 3\,[\bar{1}01]_{ccp}$, and $\mathbf{c}_{amph} = \frac{1}{2}\,[1\bar{2}1]_{ccp}$. The {111} close-packed planes of the oxygen sub-lattice coincide exactly with (100), (001), and {$\bar{2}$61} of this model amphibole (Fig. 8). Law and Whittaker (1980) note that real amphiboles are closer to the fully extended than the fully

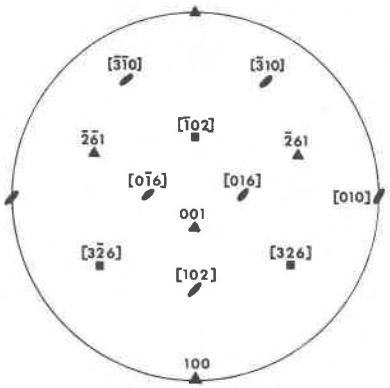

Fig. 8. The symmetry axes of a cubic close-packed oxygen array, oriented so as to correspond with the conventional stereographic setting of an amphibole. The indexing represents amphibole vectors with which the cubic close-packed axes exactly coincide in the theoretical close-packed *C2/m* amphibole structure.

rotated theoretical structures. Whereas the "model hornblende" of Figure 8 has $\beta = 109.47°$ and $|a\cos\beta| = 2c/3$ (Law and Whittaker, 1980), real hornblendes (Papike *et al.*, 1969) have $\beta \approx 105°$ and $|a\cos\beta| \approx 0.5c$. Nevertheless, the $\{111\}_{ccp}$ planes of the theoretical structure are still those with the closest approach to planar close-packing (Fig. 9), and so they are found to be planes of semi-coherence in the present study (Table 2). There is considerable misfit between ilmenite and hornblende oxygen arrays (Fig. 9), which therefore cannot be fully coherent and must have misfit dislocations in their interfaces (Fig. 5b).

The oxygen stacking sequence must change from cubic to hexagonal close-packed when hornblende is made over to ilmenite, so there would be a misfit, between cubic close-packed hexagonal close-packed oxygen arrays, across {*hki*0} prism faces of the ilmenite, even if the hornblende structure were ideally close-packed. In fact there is also a discrepancy between the oxygen-layer repeat in ilmenite ($c/6 = 2.35$Å) and the corresponding distance in hornblende (*e.g.*, Fig. 6a). For the hornblende structure depicted in Figure 9, the average distances between oxygen layers, measured normal to (100), (001), and {2̄61}, are respectively 2.38Å, 2.56Å, and 2.42Å. Therefore, considerable strain is associated with prism faces of ilmenite (Fig. 5c).

Despite the differences between the three types of orientation, none is so overwhelmingly favored as to suppress the occurrence of the others. Since two planes of the form {2̄61} are distinguishable in the observations, we have four possible (0001) planes for the ilmenite (Table 2). In each case there are two alternative sets of a_1, a_2, a_3 axes within this plane, separated by a phase-angle of 60°, giving a total of 8 distinguishable ilmenite orientations (Table 2). Because ilmenite has low symmetry (point group $\bar{3}$) arising from its cation configuration, there exists for each tabulated set of axes another set, having the reverse sign of c and a_1, a_2, a_3 in the same set of positions but reverse order. Such a pair of orientations are not equivalent by symmetry, but their oxygen arrays are indistinguishable and their diffraction patterns differ only in the intensities of some maxima. We cannot distinguish between such a pair, since intensities are unreliable in TEM (because of double diffraction) and in X-ray diffraction by inclusions (because of statistical fluctuations, from crystal to crystal, in the proportion of the ilmenite that has a particular orientation). Given the equivalence of the oxygen arrays, we do not expect one member of the pair to be markedly favored relative to the other, since there is little discrimination among orientations whose oxygen arrays *differ* in their misfits with the hornblende (Fig. 9).

In other silicate minerals it has likewise been found that oxygen packing controls the orientation in which oxide particles nucleate, during exsolution or oxidation. In olivine, the oxygens are almost exactly hexagonally close-packed with (100) as the close-packed plane, and this plane is duly shared by (0001) of ilmenite inclusions (Moseley, 1981), and {111} of spinel-group inclusions (Champness, 1970; Ashworth, 1979). The oxygen stacking sequence changes from hexagonal close-packed to cubic close-packed during the exsolution of a spinel, the reverse of the change occurring when ilmenite is formed from hornblende.

Pyroxenes are closely analogous to amphiboles, and there is a theoretical clinopyroxene structure with cubic close-packed oxygens (Law and Whittaker, 1980). Of the four possible planes, analogous to those in hornblende, on which close-packed oxides might nucleate, the only two reported are those corresponding to the (100) and (001) orientations in the amphibole. These are both found in spinel-group particles in pyroxene (Bown and Gay, 1959; Fleet *et al.*, 1980), while only the first has been reported for ilmenite (Bown and Gay, 1959; Le Maitre, 1965). Often, the morphology of oxides in pyroxene lacks any simple relation to lattice orientation. Spinel-group particles are often described as blade-like (Fleet et al., 1980), rod-like (Le Maitre,

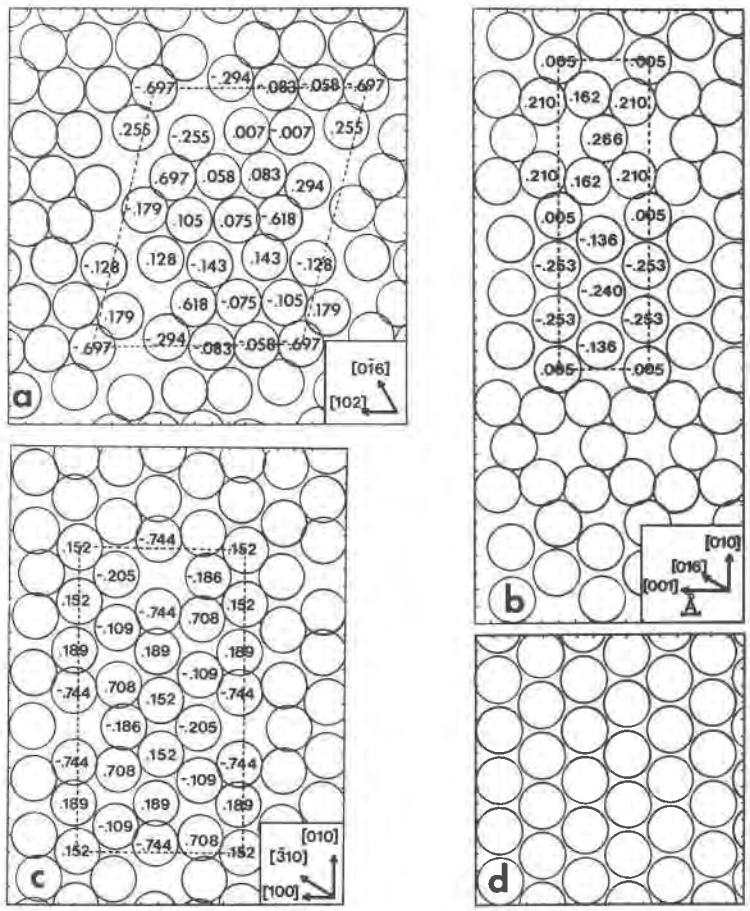

Fig. 9. The arrangements of oxygen atoms in the nearly close-packed planes of a real *C*2/*m* amphibole, generated from the unit-cell parameters and atomic co-ordinates given by Papike *et al.* (1969) for a "hornblende," actually a titanian magnesio-hastingsite (Cameron and Papike, 1979) and thus similar to the amphiboles under investigation. (a) {$\bar{2}$61}, (b) (100), (c) (001). The oxygen atoms are drawn with a nominal diameter of 2.7Å. The repeat unit is outlined. The numbers are distances, in Å, of the atom centers above and below the average plane. (d) The hexagonal arrangement in (0001) of ilmenite, for comparison.

1965), or needle-like (Elsdon, 1971; Okamura *et al.*, 1976), and ilmenite also occurs as needles (Grapes, 1975). Large (>10 μm) magnetites with consistent, irrational elongations are interpreted by Fleet *et al.* (1980) in terms of optimal phase-boundary theory (dimensional fit of the two lattices rather than the oxygen arrays). A similar effect is discernible in our largest (001)-type and (100)-type particles (Fig. 4), whose poles are systematically displaced from 001 and 100 in the sense expected from optimal phase-boundary theory (Fleet *et al.*, 1980). It is noteworthy that platy morphology on (010) of hornblende, observed on the universal stage (Fig. 4) and unrelated to oxygen packing, is similar to the blade-like (010) morphology of magnetite described by Fleet *et al.* (1980). This effect can be attributed to boundary adjustment during coarsening, but the ilmenite–hornblende boundaries in general are not fully equilibrated, as is shown by the scatter of {$\bar{2}$61}-type poles in Figure 4 and the tendency of large particles to have irregular shapes (Fig. 5d).

Rutile. Morphological elongations in pyroxene (Moore, 1968; Griffin *et al.*, 1971) do not correspond to the *c* orientations observed in hornblende (Table 3). Like the other oxides discussed above, rutile as coarse inclusions in pyroxene can have a morphology determined mutually by both phases, so that elongations are oblique to *c* (Griffin *et al.*, 1971). The smaller particles studied here are generally simpler, with elongation parallel to *c*. The particles have nucleated with this axis approximately parallel to one or another of the diads of the theoretical cubic close-packed oxygen array (Table 3; Fig. 8). These are the close-packed directions

within the close-packed planes, and this linear correspondence can be understood in terms of the linear elongation of the rutile. Evidently, the dominant control is the similarity between the oxygen repeat distance in rutile, $c = 2.96$Å, and the inter-oxygen distance in a nearly close-packed layer, which ideally would be 2.93Å but is greater, by varying amounts, in the real amphibole structure (Fig. 9). Vectors related by this tetrad in rutile are forced, by the lower symmetry of the cubic close-packed array about this axis, to occupy dissimilar environments. If one ⟨100⟩ axis of rutile coincided exactly with a triad of the cubic close-packed array, the other would not. Each of the approximate relations listed in Table 3 can be seen as a compromise between two simple orientations in which a ⟨100⟩ axis would coincide with one or other triad of Figure 8 in the plane perpendicular to *c* of the rutile. These simple orientations are those discussed by Armbruster (1981), in which a ⟨101⟩ vector as well as [001] of rutile coincides approximately with a diad of a close-packed oxygen array. The coincidence cannot be exact because the angle between the two vectors in rutile is not 60°, but approximately 57°, and various deviations from ideal relations are found in intergrowths between rutile and other oxides (Armbruster, 1981). Among the rutile particles in hornblende, it is likely that some of the orientational scatter reflects a tendency towards one or other of the simple orientations. Indeed, for one orientation of the rutile *c* axis (parallel to *b* of hornblende), we find a strong tendency for a ⟨100⟩ axis to approximate a particular triad of the cubic close-packed model, namely that represented by c^* of hornblende. This implies a close approximation between (100) of rutile and (001) of hornblende, and indicates that the latter is a better fit to the nearly close-packed plane of rutile than is (100) of the amphibole. The fit is far from perfect, as indicated by the intense strain in rutile boundaries seen in TEM.

Oxide exsolution and the amphibole structural formula

It is inferred, from the homogeneous spatial distribution of inclusions in large parts of the interiors of hornblende grains, and the close crystallographic relations between the minerals, that the inclusions grew from the hornblende in the solid state. The reactions were favored by the slow cooling of the intrusions which had been emplaced, at depth, before the end of the Caledonian regional metamorphism. There remains the question whether the reactions could occur as a simple exsolution process in a closed system. We do not observe any silicate product of exsolution. In olivine and pyroxenes, the exsolution of oxides without accompanying silicates often leads to the necessity of postulating non-stoichiometry or unusual cation coordination in the host mineral (Okamura *et al.*, 1976; Ashworth, 1979). Formation of oxide particles in pyroxene may involve open-system behavior, in particular oxidation or reduction (Garrison and Taylor, 1981).

Hornblende differs from olivine and pyroxene in the extra flexibility conferred by partition of Na between the B sites and the partly vacant A sites. The standard amphibole formula, $A_{0-1}B_2C_5^{VI}T_8^{IV}(O,OH,F,Cl)_{24}$, has 15 to 16 cations per 24 (O,OH,F,Cl). Ilmenite has a higher proportion of cations (16 per 24 O), and rutile a lower one (12). Thus, exsolution of ilmenite will cause the cation total in the remaining hornblende to decrease, so that Na should move from A to the B sites to keep the latter full, while exsolution of rutile will have the reverse effect. More generally, if a fraction I is made over to ilmenite and R to rutile, leaving $(1–I–R)$ as hornblende, then the original Fe and Ti contents of hornblende change to Fe′ and Ti′ thus:

$$\mathrm{Fe}' = (\mathrm{Fe}–8I)$$

$$\mathrm{Ti}' = (\mathrm{Ti}–8I–12R).$$

Of the 15 atoms that occupied the B, C, and T sites before exsolution, there remain $(15–16I–12R)$, to $24(1–I–R)$ anions. For all these sites to remain fully occupied, the amount of Na that should move from A to B sites is

$$\Delta\mathrm{Na}^{\mathrm{B}} = 15\,(1–I–R) – (15–16I–12R)$$

$$= I–3R,$$

which is zero if ilmenite and rutile are exsolved in the ratio 3:1. In the hornblendes studied, this ratio is not found, and Na^{B} is expected to change; however, the effect will be slight and may be undetectable in electron microprobe analysis. To produce a change, per amphibole formula unit, of 0.15 (1% of the B + C + T total) would require that approximately 5% of the oxygen atoms be made over to rutile or 13% to ilmenite, larger quantities than we observe. For exsolution of 2.8% ilmenite and negligible rutile (as estimated in the Glen Scad-

dle amphibole), $\Delta Na^B = 0.03$, which is smaller than the likely analytical errors. Thus, movement of Na to this extent is accepted as possible.

Some Al must move from four-fold to six-fold coordination, in order that the T^{IV} total remains 8:

$$\Delta Al^{VI} = -\Delta Al^{IV} = 8(I + R).$$

The increasing proportion of (OH,F,Cl) ions can continue to be accommodated if the original amphibole had less than 2 of these per formula unit, or if solid solution towards a hydroamphibole end-member is possible. The cation total reaches 16 when $4R$ becomes equal to the original number of vacant A sites.

In summary, exsolution of rutile and ilmenite from hornblende is possible, without introducing excess ions or vacancies relative to the standard amphibole structure, provided that: (1) the initial hornblende has at least $4R$ vacancies in the A sites; (2) the initial hornblende has at least $8(I + R)$ Al ions in the T^{IV} sites; and (3) $(I - 3R)$ Na atoms can move from the A to the B sites.

Restriction (3) seems the most severe in amphiboles of the type studied here; if we are correct in arguing that Fe^{3+} is low, then the analyses indicate very little Na in the B sites either before or after exsolution, *i.e.*, very restricted solid solution towards a sodic calcic amphibole end-member under the conditions experienced by these amphiboles.

Conclusions

In the rocks studied, ilmenite and rutile particles formed inside hornblende by a process of nucleation and growth from the primary amphiboles, which were probably titanian ferroan pargasites. The reaction occurred during the slow cooling of the Caledonian terrane from regional metamorphic temperatures. The consequences for the amphibole structural formula are slight. The analytical data are consistent with exsolution in a closed system, accompanied by adjustments in site occupancies within the amphibole, some Al moving from the T^{IV} to the C^{VI} sites, and some Na moving between the A and B sites. Because of the vacancies in the A sites, the crystal chemistry of hornblende can accommodate exsolution of oxides more readily than can the pyroxene or olivine structures.

The orientations of the oxide minerals were controlled by nucleation in a semi-coherent relation to the hornblende lattice. Packing of oxygen atoms determines the orientation of (0001) of ilmenite and c of rutile. The morphology of small particles is simply related to their lattices, but the coarser particles lost their simple shapes as they grew, presumably thus reducing the strain energy associated with the oxide–hornblende interfaces. The observations suggest that the clouding of amphiboles by opaque particles may often be due to the exsolution of Ti-rich oxide minerals during cooling, as the stable extent of Ti substitution in the amphibole decreases with decreasing temperature.

Acknowledgments

We are indebted to the following for facilities and advice: Dr. M. H. Loretto, Birmingham University (high-voltage TEM); Mr. R. G. Howell, Dr. S. Murphy, and Dr. W. B. Hutchinson, Department of Metallurgy and Materials Engineering, Aston (electron microprobe and SEM); Dr. A. E. McCarthy, Department of Chemistry, Aston (X-ray oscillation camera); and Miss G. Thomas, Department of Civil Engineering, Aston (digitizer and associated microcomputer). We thank Dr. D. J. Vaughan for criticizing a draft.

References

Armbruster, Th. (1981) On the origin of sagenites: structural coherency of rutile with hematite and spinel structure types. Neues Jahrbuch für Mineralogie Monatshefte, 328–334.

Ashworth, J. R. (1979) Two kinds of exsolution in chondritic olivine. Mineralogical Magazine, 43, 535–538.

Bard, J. P. (1970) Composition of hornblendes formed during the Hercynian progressive metamorphism of the Aracena metamorphic belt (SW Spain). Contributions to Mineralogy and Petrology, 28, 117–134.

Bown, M. G. and Gay, P. (1959) The identification of oriented inclusions in pyroxene crystals. American Mineralogist, 44, 592–602.

Cameron, M. and Papike, J. J. (1979) Amphibole crystal chemistry: A review. Fortschritte der Mineralogie, 57, 28–67.

Champness, P. E. (1970) Nucleation and growth of iron oxides in olivines, $(Mg,Fe)_2SiO_4$. Mineralogical Magazine, 37, 790–800.

Drever, H. I. (1940) The geology of Ardgour, Argyllshire. Transactions of the Royal Society of Edinburgh, 60, 141–170.

Elsdon, R. (1971) Clinopyroxenes from the Upper Layered Series Kap Edvard Holm, East Greenland. Mineralogical Magazine, 38, 49–57.

Fleet, M. E., Bilcox, G. A., and Barnett, R. L. (1980) Oriented magnetite inclusions in pyroxenes from the Grenville Province. Canadian Mineralogist, 18, 89–99.

Garrison, J. R., Jr. and Taylor, L. A. (1981) Petrogenesis of pyroxene–oxide intergrowths from kimberlite and cumulate rocks: co-precipitation or exsolution. American Mineralogist, 66, 723–740.

Grapes, R. H. (1975) Petrology of the Blue Mountain Complex, Marlborough, New Zealand. Journal of Petrology, 16, 371–428.

Griffin, W. L., Jensen, B. B., and Misra, S. N. (1971) Anomalously elongated rutile in eclogite–facies pyroxene and garnet. Norsk Geologisk Tidsskrift, 51, 177–185.

Hall, M. G. and Lloyd, G. E. (1981) The SEM examination of geological samples with a semiconductor back-scattered electron detector. American Mineralogist, 66, 362–368.

Hatch, F. H., Wells, A. K., and Wells, M. K. (1972) Petrology of the Igneous Rocks, 13th edition. Thomas Murby, London.

Helz, R. T. (1973) Phase relations of basalts in their melting range at P_{H_2O} = 5kb as a function of oxygen fugacity. Part I. Mafic phases. Journal of Petrology, 14, 249–302.

Institute of Geological Sciences (1975) Geological Survey of Great Britain (Scotland) 1:50 000 Solid Edition Sheet 62E: Loch Lochy.

Lally, J. S., Heuer, A. H., and Nord, G. L., Jr. (1976) Precipitation in the ilmenite–hematite system. In H.-R. Wenk, Ed., Electron Microscopy in Mineralogy, p. 214–219. Springer-Verlag, Berlin.

Law, A. D. and Whittaker, E. J. W. (1980) Rotated and extended model structures in amphiboles and pyroxenes. Mineralogical Magazine, 43, 565–574.

Leake, B. E. (1965) The relationship between composition of calciferous amphibole and grade of metamorphism. In W. S. Pitcher and G. W. Flinn, Eds., Controls of Metamorphism, p. 299–318. Oliver and Boyd, Edinburgh.

Leake, B. E. (1978) Nomenclature of amphiboles. American Mineralogist, 63, 1023–1052.

Le Maitre, R. W. (1965) The significance of the gabbroic xenoliths from Gough Island, South Atlantic. Mineralogical Magazine, 34, 303–317.

Moore, A. (1968) Rutile exsolution in orthopyroxene. Contribution to Mineralogy and Petrology, 17, 233–236.

Moseley, D. (1981) Ilmenite exsolution in olivine. American Mineralogist, 66, 976–979.

Okamura, F. P., McCallum, I. S., Stroh, J. M., and Ghose, S. (1976) Pyroxene–spinel intergrowths in lunar and terrestrial pyroxenes. Proceedings of the Seventh Lunar Science Conference, 1889–1899.

Papike, J. J., Ross, M., and Clark, J. R. (1969) Crystal-chemical characterization of clinoamphiboles based on five new structure determinations. Mineralogical Society of America Special Paper 2, 117–136.

Raase, P. (1974) Al and Ti contents of hornblende, indicators of pressure and temperature of regional metamorphism. Contributions to Mineralogy and Petrology, 45, 231–236.

Stoker, M. S. (1980) The geology of eastern Ardgour. Ph.D. Thesis, Liverpool University.

Stout, J. H. (1972) Phase petrology and mineral chemistry of coexisting amphiboles from Telemark, Norway. Journal of Petrology, 13, 99–145.

Thompson, J. B., Jr. (1970) Geometrical possibilities for amphibole structures: model biopyriboles. American Mineralogist, 55, 292–293.

Manuscript received, March 11, 1982;
accepted for publication, July 6, 1982.